A Damage Tolerance Comparison of Composite Hat-Stiffened and Honeycomb Sandwich Structure for Launch Vehicle Interstage Applications

A.T. Nettles
Marshall Space Flight Center, Huntsville, Alabama

The NASA STI Program…in Profile

Since its founding, NASA has been dedicated to the advancement of aeronautics and space science. The NASA Scientific and Technical Information (STI) Program Office plays a key part in helping NASA maintain this important role.

The NASA STI Program Office is operated by Langley Research Center, the lead center for NASA's scientific and technical information. The NASA STI Program Office provides access to the NASA STI Database, the largest collection of aeronautical and space science STI in the world. The Program Office is also NASA's institutional mechanism for disseminating the results of its research and development activities. These results are published by NASA in the NASA STI Report Series, which includes the following report types:

- TECHNICAL PUBLICATION. Reports of completed research or a major significant phase of research that present the results of NASA programs and include extensive data or theoretical analysis. Includes compilations of significant scientific and technical data and information deemed to be of continuing reference value. NASA's counterpart of peer-reviewed formal professional papers but has less stringent limitations on manuscript length and extent of graphic presentations.

- TECHNICAL MEMORANDUM. Scientific and technical findings that are preliminary or of specialized interest, e.g., quick release reports, working papers, and bibliographies that contain minimal annotation. Does not contain extensive analysis.

- CONTRACTOR REPORT. Scientific and technical findings by NASA-sponsored contractors and grantees.

- CONFERENCE PUBLICATION. Collected papers from scientific and technical conferences, symposia, seminars, or other meetings sponsored or cosponsored by NASA.

- SPECIAL PUBLICATION. Scientific, technical, or historical information from NASA programs, projects, and mission, often concerned with subjects having substantial public interest.

- TECHNICAL TRANSLATION. English-language translations of foreign scientific and technical material pertinent to NASA's mission.

Specialized services that complement the STI Program Office's diverse offerings include creating custom thesauri, building customized databases, organizing and publishing research results…even providing videos.

For more information about the NASA STI Program Office, see the following:

- Access the NASA STI program home page at <http://www.sti.nasa.gov>

- E-mail your question via the Internet to <help@sti.nasa.gov>

- Fax your question to the NASA STI Help Desk at 443–757–5803

- Phone the NASA STI Help Desk at 443–757–5802

- Write to:
  NASA STI Help Desk
  NASA Center for AeroSpace Information
  7115 Standard Drive
  Hanover, MD 21076–1320

A Damage Tolerance Comparison of Composite Hat-Stiffened and Honeycomb Sandwich Structure for Launch Vehicle Interstage Applications

A.T. Nettles
Marshall Space Flight Center, Huntsville, Alabama

TABLE OF CONTENTS

LIST OF FIGURES

LIST OF TABLES

TECHNICAL MEMORANDUM

A DAMAGE TOLERANCE COMPARISON OF COMPOSITE HAT-STIFFENED AND HONEYCOMB SANDWICH STRUCTURE FOR LAUNCH VEHICLE INTERSTAGE APPLICATIONS

1. INTRODUCTION

An interstage structure on a launch vehicle is a cylindrical structure that separates various stages of the vehicle. By utilizing carbon fiber composites instead of aluminum, it is hoped that the mass of the structure can be reduced. These structures are dominated by compression stresses and can either be stiffness (buckling) or strength critical. Two methods of obtaining a strong and stiff cylinder are by using sandwich construction or stringer-stiffened structure. Sandwich construction consists of using a lightweight core between two composite face sheets. The composite face sheets are designed to carry the structural compressive load and the core serves to distribute stresses via shear to the two face sheets such that the cross section of the structure has a high moment of inertia and thus high buckling load.

The stringer-stiffened concept utilizes one face sheet that has long, narrow sections with a constant prismatic cross section placed in the direction of loading at discreet intervals along the width of the part. The stringer adds stability to the face sheet to help prevent buckling. A common shape for the prismatic cross section of the stiffeners is a trapezoid whose cross section resembles a hat and thus the term 'hat stiffener.' These two concepts are shown schematically in figure 1.
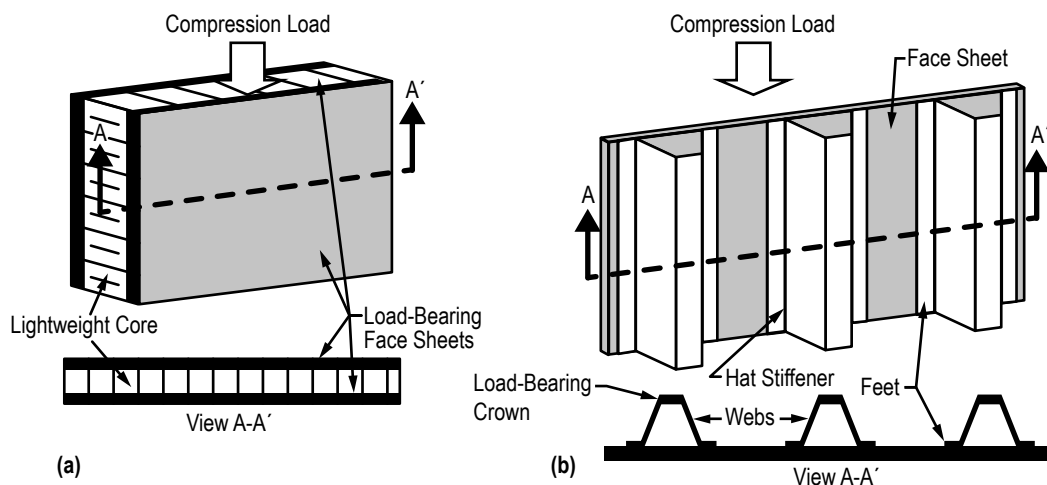

Figure 1. Concepts for carrying large compressive loads: (a) Sandwich and (b) hat stiffened.

The compressive failure mechanism differs in these two structures in that the hat-stiffened panel can have its face sheet buckle and still carry significant load through the hat stiffeners. Once the face sheet of a sandwich structure begins to buckle, catastrophic failure typically occurs. Thus, some of the load-carrying capability of the hat-stiffened structure is in the face sheet postbuckling regime.

For most structural launch vehicle applications, the composite part must be designed under damage tolerance considerations. The two types of structural concepts shown in figure 1 can have greatly different damage tolerance characteristics. The sandwich structure is uniform across its acreage and thus any impact from a foreign object will have essentially the same response regardless of where the impact takes place. The hat-stiffened concept, on the other hand, is not uniform across its acreage and will have a different response if impacted by a foreign object, depending on where the impact takes place. For example, an impact on the face sheet between hat stiffeners will behave differently than an impact directly on one of the hat stiffeners. This is very important as the hat stiffeners are on the outside of the cylinder for interstage structure and are thus more prone to accidental impacts from foreign objects.

There are two major modes of failure for compression-loaded composite structures—global buckling of the structure and ply level microbuckling (material failure). The effects of damage to global buckling have been examined and are mostly in the form of debonded stringers.[1] However, impact damage is also a concern to a composite structure since such damage can cause the composite material to lose much of its load-carrying capability; i.e., the laminate will experience microbuckling at a lower load than had it not been impacted.

Impact damage to composite sandwich structures has been reviewed in detail elsewhere;[2] however, the literature is sparser with regards to impact damage of hat-stiffened composite structures. One of the first studies on the effects of impact damage on hat-stiffened panels[3] showed that impacts in the high stiffness regions—crown and face sheet behind crown—of the panel could cause a significant drop in compressive load-carrying capability for a structure designed to carry a line load of 9,000 lb/in. It was determined that impact damage in the low stiffness regions—the web and face sheet between hats—did not cause a significant decrease in compressive load-carrying capability. It was also shown that hat-stiffened panels designed for lower load-carrying capabilities (3,000 lb/in) did not suffer compressive strength degradation, even when impacted in the high stiffness regions.

Foam-filled, hat-stiffened panels designed for a load-carrying capability of 3,000 lb/in were evaluated in reference 4 and it was determined that impact to the crown had little effect on residual compressive load-carrying capability, but impact to the face sheet behind the crown, or at the crown face sheet interface region caused drops in compressive load-carrying capability. A related study using carbon fabric and resin transfer molding to manufacture hat-stiffened panels was examined in reference 5. The damage tolerance of the hat-stiffened panels in this study was increased by stitching the hat stringers to the face sheet. Results showed that damage tolerance was increased over panels made from preimpregnated, unidirectional tape, mainly due to the through-thickness reinforcements (stitching) at the hat/face sheet interface, preventing the stringer from debonding from the face sheet.

It has been noted that for a skin-stringer structure, the failure mechanism consists of a series of buckles in the face sheet which result in the load being transferred to the stiffeners which eventually leads to a material compressive failure (ply level microbuckling) in the stiffeners.[6] This reference also suggests that a three-stringer panel be used for compression after impact testing since a stringer and two adjacent skin bays would represent the structure and the two stringers at the ends of the panel would replicate the boundary conditions of the actual structure. However, by having to test a panel of this size, more material and a larger capacity loading frame would be needed. It would be simpler to test a smaller specimen, such as a single stringer, and extrapolate the data to multistringer panels. This has been attempted with some success[7] but finite element analysis is needed to size the single stringer specimen to replicate its behavior in a multistringer panel.

In this current study, two stringer panels were tested since that was the only structure available for damage tolerance testing. While certainly not ideal for design purposes, the two stringer panels were deemed sufficient to use for a simple comparison with sandwich structure.

It is the intent of this study to ascertain the criticality of impact damage to hat-stiffened composite panels that are designed to be used as a launch vehicle interstage. The major thrust of this study will focus on the criticality of the location of impact rather than the severity of impact. These data are then compared to compression after impact data from sandwich specimens also designed for use for a launch vehicle interstage.

2. MATERIALS AND TESTING

2.1 Sandwich Structure

The sandwich specimens consisted of composite panels that were manufactured by a co-cure process. The honeycomb core used was perforated 5052 aluminum with a density of 3.1 lb/ft^3 and a thickness of 1.125 in. The face sheets consisted of IM7/8551-7 carbon/epoxy and the film adhesive used to bond the face sheet to the core was FM-300k with an areal density of 0.08 lb/ft^2. The layup of the face sheet was [45, 0, –45, 0, 90, 0, 0, 90, 0]$_S$. Each face sheet had a thickness of 0.10 in. The layup of the face sheet is the same as that scheduled to be used on full-scale hardware. The panels were manufactured as 24- by 2-in-square sandwich plates. All panels were subjected to nondestructive evaluation (NDE) using infrared thermography (IRT) testing to ensure no flaws were present before specimens were machined from the panels. From the 24- by 24-in panels, 4- by 6-in specimens were machined for impact and subsequent compression testing. This gave each specimen a load-bearing, cross-sectional area of 0.80 in^2 which was used to calculate the breaking stresses.

After impact, the specimens were inspected with IRT after which the specimens were prepared for end-loaded compression testing. In order to avoid premature failures due to end brooming, the loaded ends of the specimen were potted with epoxy in an aluminum frame and machined to a tolerance of ±0.001 in parallelism. Details of the specimen geometry and testing methodology are published elsewhere.[8]

2.2 Hat-Stiffened Structure

The hat-stiffened structure evaluated in this study was made from T40-800/5320 carbon/epoxy unidirectional prepreg and consisted of two hat stiffeners. The hat-stiffened panels where manufactured utilizing out-of-autoclave techniques. The layup of the face sheet portion of the hat-stiffened panels was 17-ply [90$_2$, 0, 90, 45, –45, 0$_2$, 90$_{bar}$]$_S$ which gives the face sheet a layup with 35% 0° plies. The webs and feet had a layup of [45, –45]$_S$ and the crown consisted of [0$_4$, 45, 0$_4$,–45, 0, 0$_{bar}$]$_S$ (83% 0° plies). The web, crown, and feet all had an outer ply of fabric placed at ±45°. A gap inevitably forms between the inner two radii of each hat stiffener and the face sheet. A preformed epoxy rod was used as a gap filler and is referred to as a noodle. Some of the hat stiffeners were precured and then co-bonded to the face sheet in a secondary bonding operation. Most of the hat-stiffened specimens were manufactured with the hat stringer co-cured to the face sheet. Figure 2 shows a schematic of the type of specimen and the nomenclature that is used to describe them throughout this Technical Memorandum.

The hat-stiffened specimens were impacted using a drop-weight instrumented impact test apparatus. The locations of the impact on the hat-stiffened specimens were varied with the incident impact energy being held fairly constant. The impact energy used was similar to those used for comparable sandwich structure specimens. This was done to determine the criticality of location of impact on the hat-stiffened specimens. All of the impactors had spherically shaped ends, most with a 0.5-in diameter.
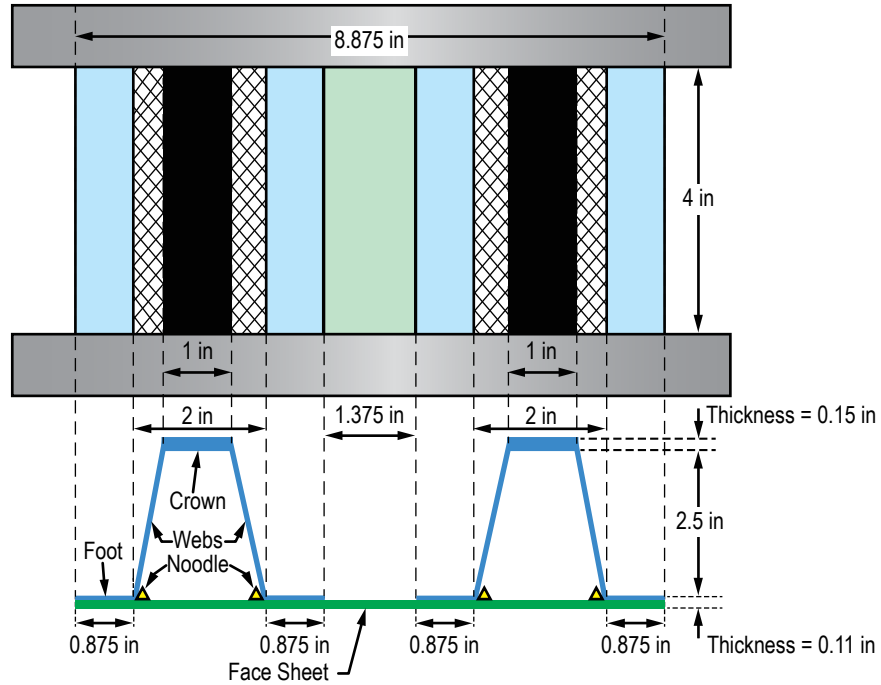
Figure 2. Double hat-stiffened specimen.

After impact testing, the specimens were assessed for damage using IRT. This NDE technique utilizes a burst of heat from a quartz lamp and a very sensitive infrared camera monitors the dissipation of heat from the specimen. The heat will emit at a different rate at locations where damage exists and the infrared camera shows these areas (termed 'indications') on a digital computer. An example of an IRT indication is shown in figure 3.
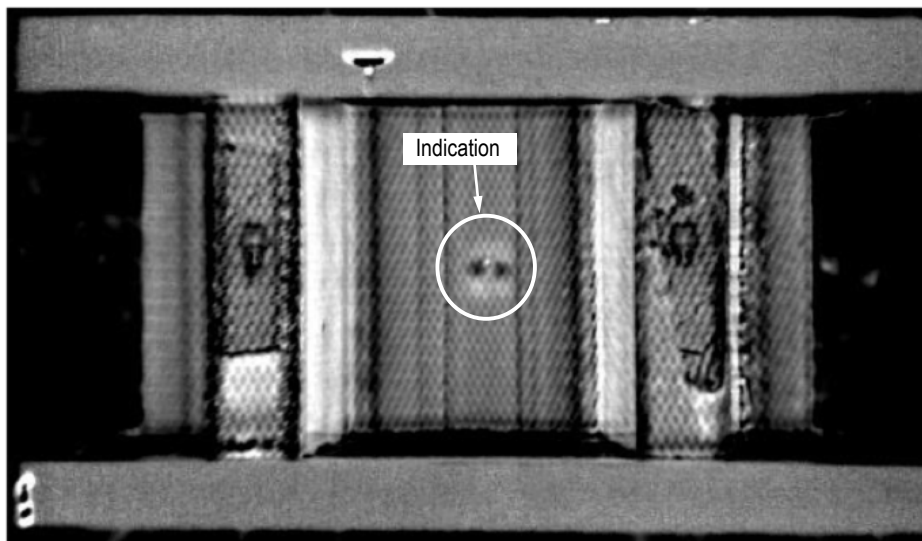

Figure 3. Example of an IRT indication on an impacted specimen.

The impacted specimens were mounted with strain gauges at the front and rear of each specimen as shown schematically in figure 4. These gauges were to ensure even loading of the specimen during testing. If the gauges differed by more than 10%, the test was stopped and shims were placed between the upper platen and the load cell until uniform loading was achieved.
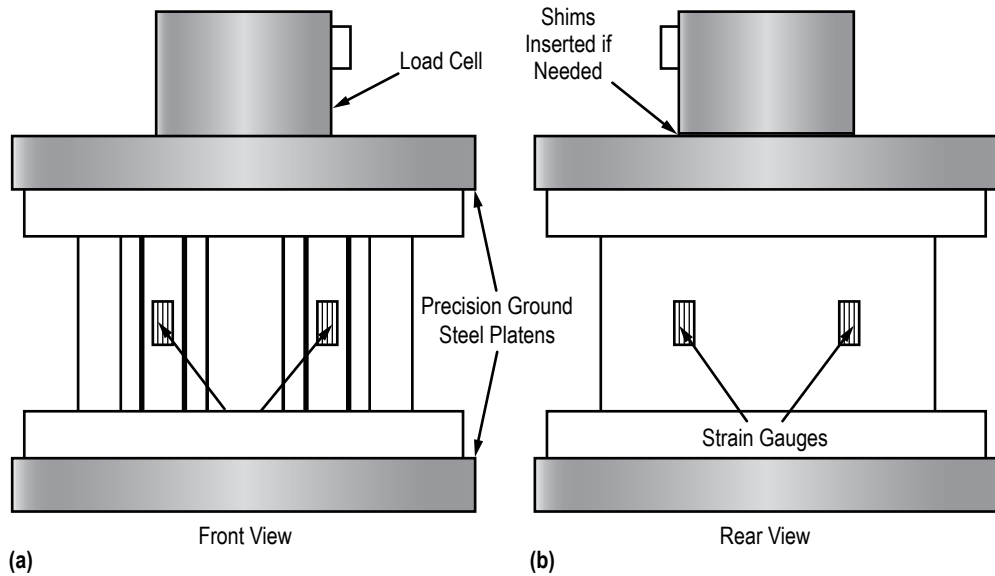

Figure 4. Compression test of hat-stiffened specimens: (a) Front view and (b) rear view.

The edges of the specimen were free and not supported. A 100-kip load frame was used with a test rate of 0.05 in/min. Each test was recorded with a digital video camera for subsequent analysis. Any face sheet buckling that occurred was only assessed visually. Ideally, back-to-back strain gauges would be placed at the center of the face sheet and monitored for divergence from each other; however, limited strain gauges for this study did not allow for this. Since the main measurement of concern was ultimate load-carrying capability, the buckling of the face sheets was not assessed in detailed.

3. RESULTS

3.1 Hat-Stiffened Structure

The results will be presented individually since each specimen—with a few exceptions—had a different impact location and/or energy that resulted in some differing compression-after-impact (CAI) results. The specimen nomenclature used was 'double #' where 'double' indicated two hat stiffeners per specimen and '#' was a numerical designation for each specimen.

3.1.1 Double 1

This specimen had hat stiffeners that were precured and then bonded to the face sheet in a secondary bonding operation. This specimen was not impacted. As it was loaded, buckling of the face sheet was noted beginning at ≈40 kips. At 55 kips, there appeared to be a disbond between a foot of a hat and the face sheet. Catastrophic failure occurred at 66.6 kips. Figure 5 shows the hat stiffener/face sheet disbond and the specimen just after catastrophic failure.
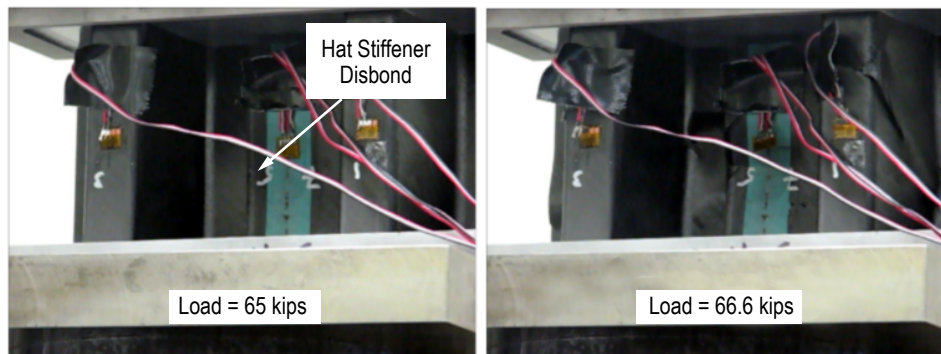

Figure 5. Hat stiffener/face sheet disbond and total failure of specimen double 1.

3.1.2 Double 2

This specimen had hat stiffeners that were precured and then bonded to the face sheet in a secondary bonding operation. The specimen was impacted on the foot of a web, towards the center of the specimen, with a 0.5-in-diameter impactor at impact energy of 5.5 ft-lb as shown schematically in figure 6.
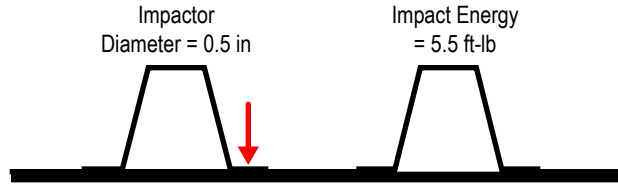
Figure 6. Location of impact on specimen double 2.

A photograph of an IRT image of the impacted specimen is presented in figure 7. It appears that a 3.4-in length ('length' defined as in the direction of loading) of the foot has disbonded from the face sheet. This disbond does not span the entire width of the foot and has a maximum width of 0.6 in (the foot bond has a width of 0.875 in). Thus, about 70% of the width of one of the feet on one of the hat stiffeners has disbonded due to the impact event.
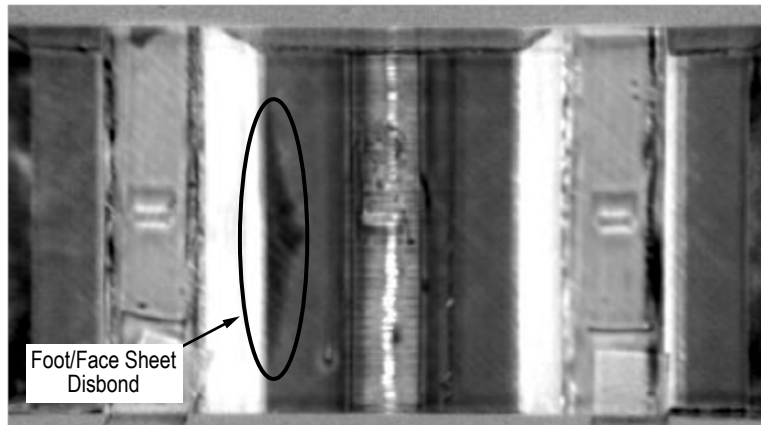

Figure 7. IRT for specimen double 2.

Upon loading, the disbond between the foot and face sheet grew steadily, in a width-wise direction, starting at 30 kips. The disbond grew across the width of the foot, and at 46 kips, an audible pop occurred. Photographs of the specimen near the beginning of the test and at 46 kips are shown in figure 8.

8
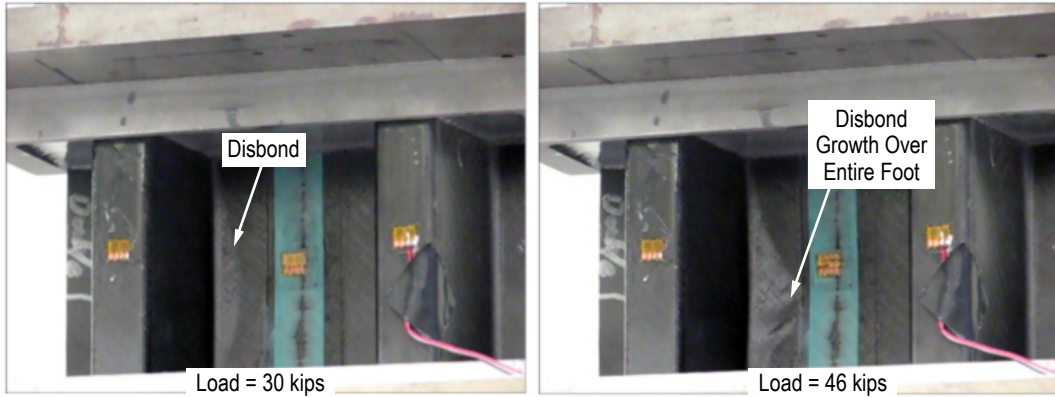
Figure 8. Hat stiffener/face sheet disbond growth on specimen double 2.

With further loading, catastrophic failure occurred at 58.1 kips. Catastrophic failure is defined in this study as total collapse of the face sheet and both hat stringers with no discernable time between collapse of these components of the structure. Catastrophic failure implies that the specimen could no longer carry any load. A photograph of the specimen just after failure is shown in figure 9.
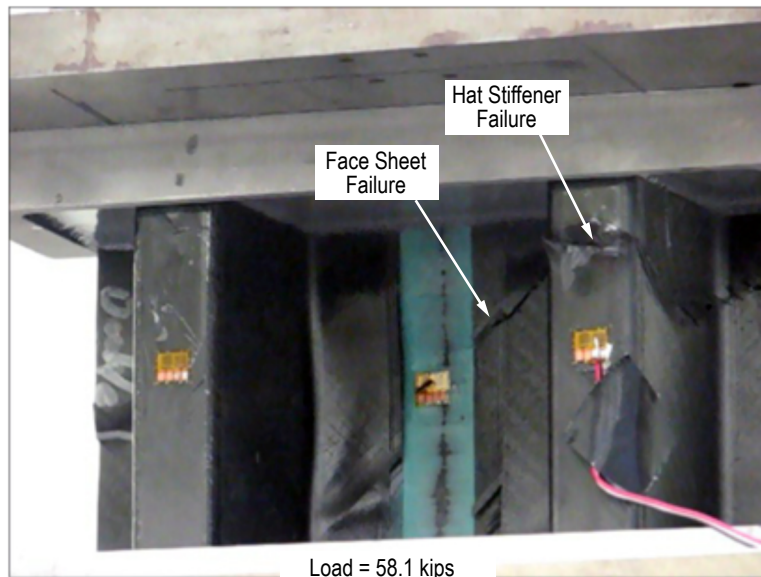

Figure 9. Failure of specimen double 2.

3.1.3 Double 3

This specimen had hat stiffeners that were precured and then bonded to the face sheet in a secondary bonding operation. This specimen was impacted at the center of the specimen, directly onto the face sheet between the two hats, with a 0.5-in-diameter impactor with an impact energy of 5.6 ft-lb as shown schematically in figure 10.
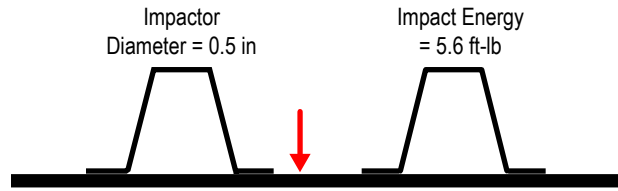
Figure 10. Location of impact on specimen double 3.

A photograph of an IRT image of the impacted specimen is presented in figure 11. A relatively small indication suggests that there are one or more circular delaminations within the face sheet with an overall size of ≈0.5-in diameter.
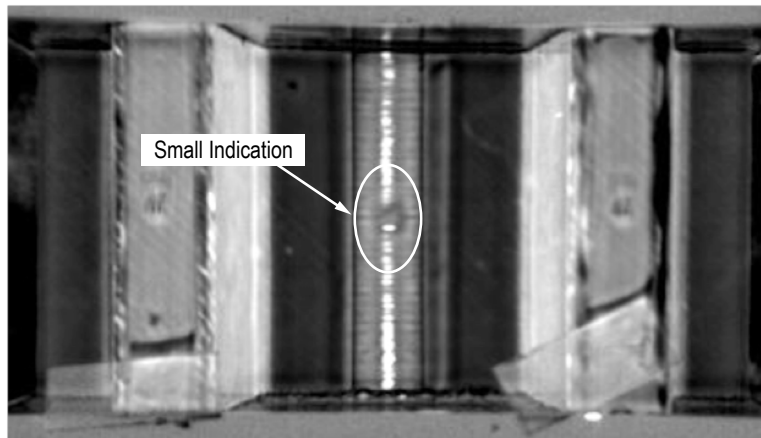

Figure 11. IRT for specimen double 3.

The specimen was loaded to 58.7 kips at which catastrophic failure occurred. This is the same load magnitude at which specimen double 1 failed, indicating that the foot/face sheet disbond did not greatly lower the compressive load-carrying capability of the structure, compared to when the face sheet has slight damage.

3.1.4 Double 4

This specimen had hat stiffeners that were precured and then bonded to the face sheet in a secondary bonding operation. The specimen was impacted on the foot of one of the webs with a 1.5-in-diameter impactor with an impact energy of 6.3 ft-lb as shown schematically in figure 12. This is a similar impact to that on specimen double 1 except that a larger impactor with 14% more energy was used.
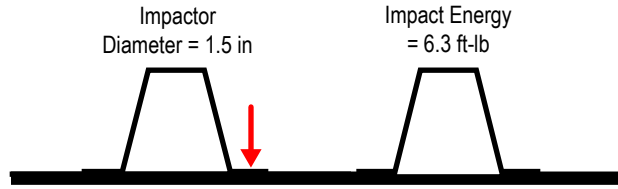
Figure 12. Location of impact on specimen double 4.

A photograph of an IRT image of the impacted specimen is presented in figure 13. The indication shows damage about 1.6 inches in length and spanning 80% of the width of the foot. Although this specimen was hit with more impact energy than specimen double 2, the length of the disbond between the foot and face sheet was about one-half that of specimen double 2.
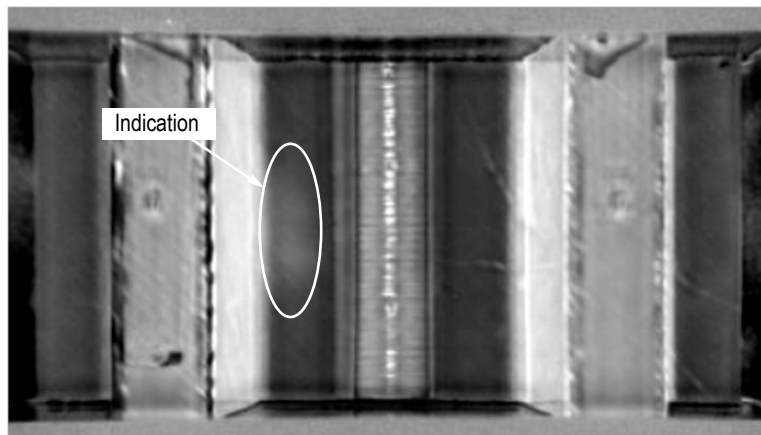

Figure 13. IRT for specimen double 4.

The specimen exhibited disbonding of the impacted foot section from the face sheet at 40 kips. This disbond appears to go beyond the foot of the hat stiffener and extends into the face sheet of the specimen. Figure 14 shows a photograph of the specimen just after this disbond has occurred. Apparently the disbond seen in the IRT image is in the face sheet itself rather than at the hat/face sheet bond as it was in specimen double 2. Thus, the larger diameter impactor perhaps changed the damage morphology.
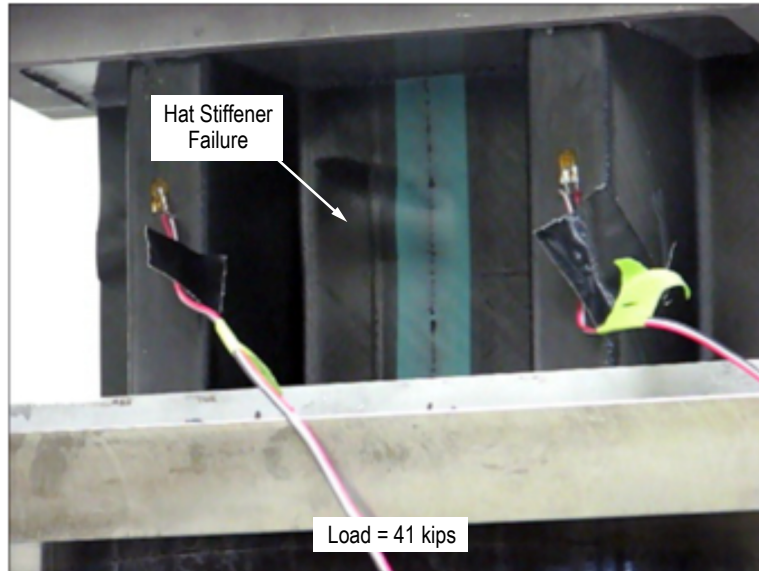
Figure 14. Hat stiffener disbond of specimen double 4.

At 44.4 kips, the load fell suddenly to ≈20 kips as the large delamination propagated across the face sheet of the specimen from the original delamination that was seen at 40 kips (fig. 14). Testing was stopped at this point. A photograph of the specimen after the large delamination has formed across the entire face sheet is shown in figure 15.
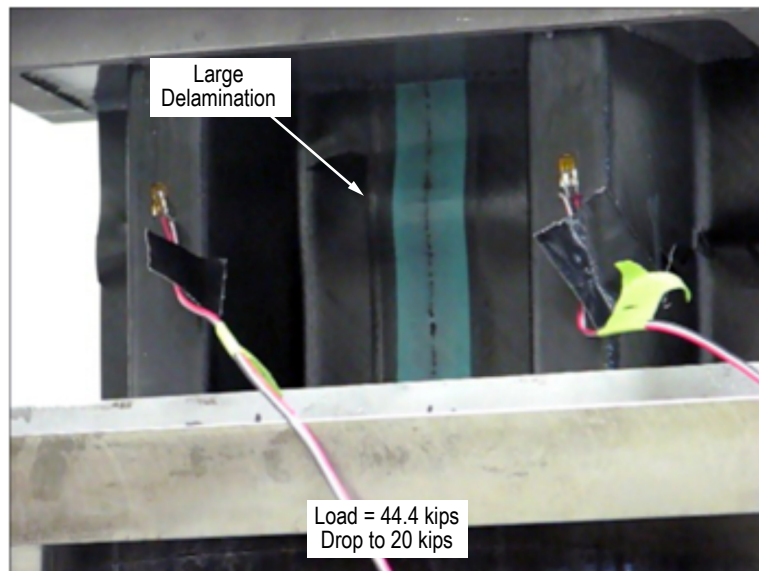

Figure 15. Delamination across entire face sheet of specimen double 4.

3.1.5 Double 5

This specimen had hat stiffeners that were precured and then bonded to the face sheet in a secondary bonding operation. This specimen was impacted on the face sheet directly behind a crown with a 0.5-in-diameter impactor with an impact energy of 10 ft-lb as shown schematically in figure 16.
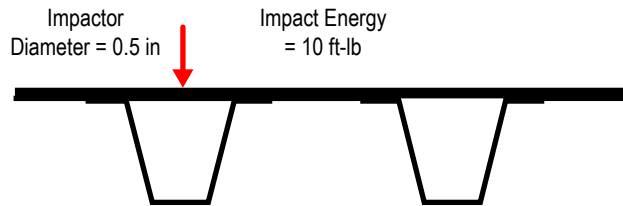

Figure 16. Location of impact on specimen double 5.

A photograph of an IRT image of the impacted specimen is presented in figure 17. The impact caused a circular area of damage ≈1 inch in diameter.
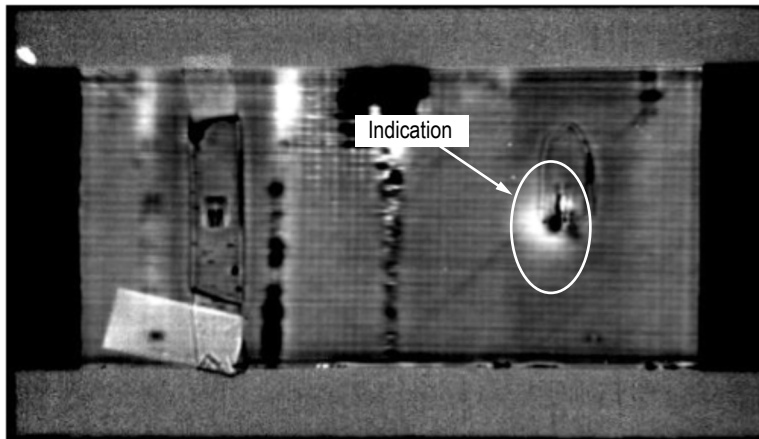

Figure 17. IRT for specimen double 5.

The specimen exhibited dimpling of the face sheet at the impact location beginning at ≈45 kips. At a load of 51.2 kips, the face sheet failed from the impact zone but the hat stiffeners remained intact. After failure, the specimen was able to carry a load of 25 kips. The face sheet dimpling and face sheet failure are shown in figure 18.
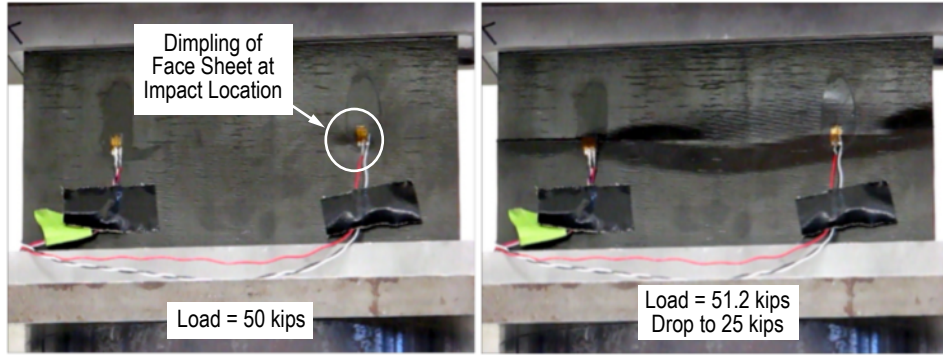
Figure 18. Dimpling at impact site and face sheet failure of specimen double 5.

3.1.6 Double 6

This specimen, and all subsequent specimens, had hat stiffeners that were co-cured to the face sheet in a single cure/bonding operation. This specimen was impacted at the center of one of the crowns with a 0.5-in-diameter impactor with an impact energy of 5.9 ft-lb as shown schematically in figure 19.
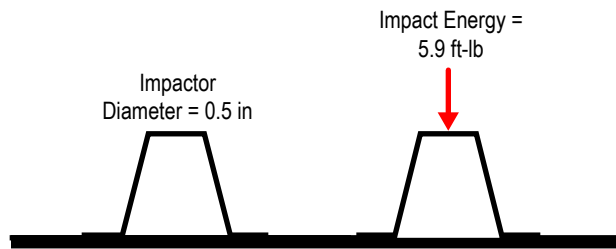
Figure 19. Location of impact on specimen double 6.

A photograph of an IRT image of the impacted specimen is presented in figure 20. The image suggests damage about 1 in long and spanning 60% of the width of the crown.
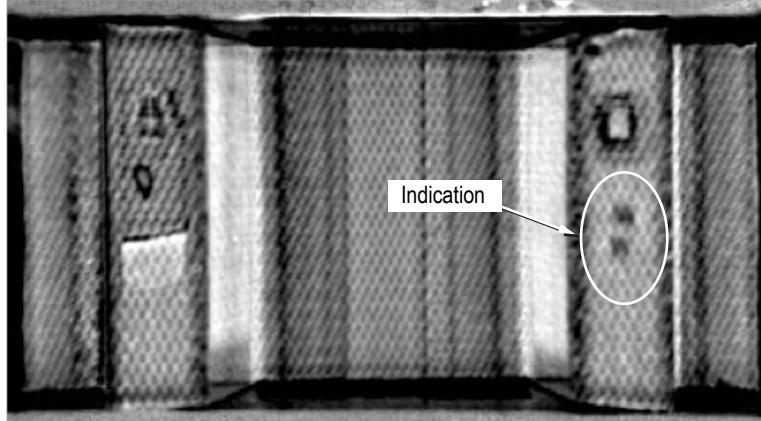
Figure 20. IRT for specimen double 6.

The specimen exhibited a loud pop at 57.9 kips which consisted of failure of the impacted crown as shown in figure 21.
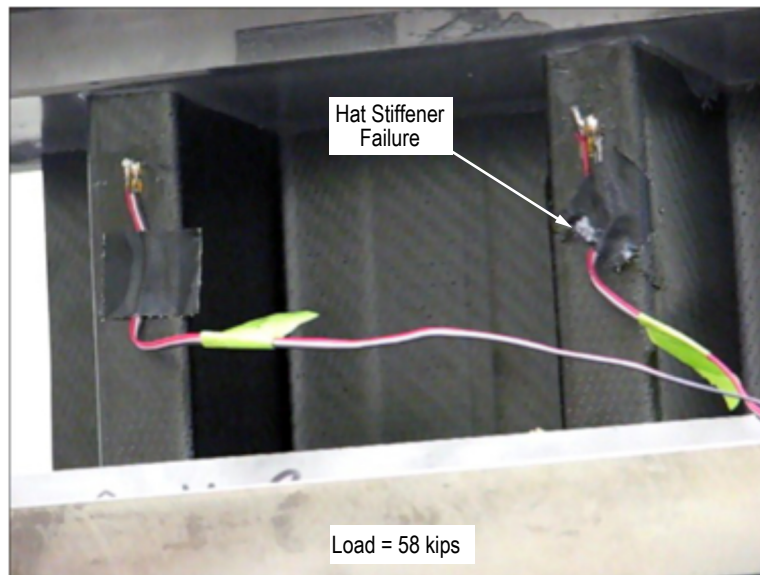
Figure 21. Hat stiffener failure of specimen double 6.

Buckling of the face sheet was apparent at ≈70 kips and the specimen failed in a cata-strophic manner at 84.7 kips. Photographs of these two events are shown figure 22.
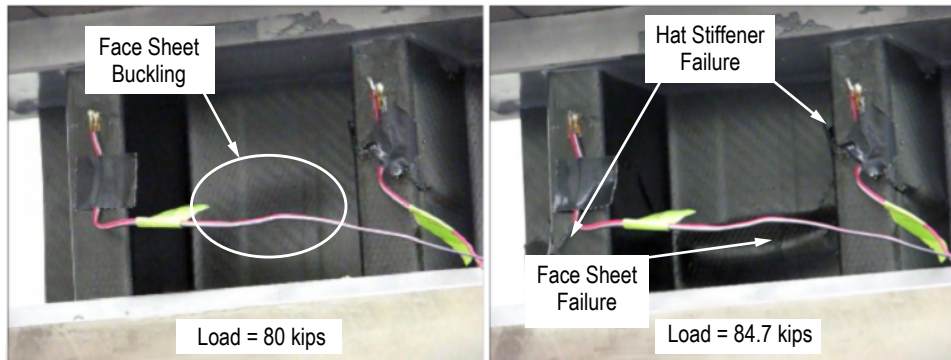
Figure 22. Buckling and catastrophic failure of specimen double 6.

3.1.7 Double 7

This specimen was impacted at the intersection of the web/crown area of one of the hat stiffeners with a 1.5-in-diameter impactor with an impact energy of 7.7 ft-lb as shown schemati-cally in figure 23. This was to determine if the location of impact on the crown was a critical parameter by comparison to specimen double 6.
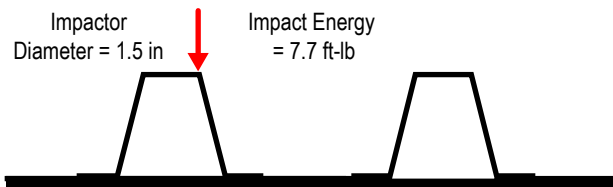
Figure 23. Location of impact on specimen double 7.

A photograph of an IRT image of the impacted specimen is presented in figure 24. The indication is difficult to see due to the web of the hat stiffener being under the impact site. This changes the damage morphology as well as gives a different IRT signature as can be noted on all of the other specimens that show 'nonuniformity' at the edges of the crown.
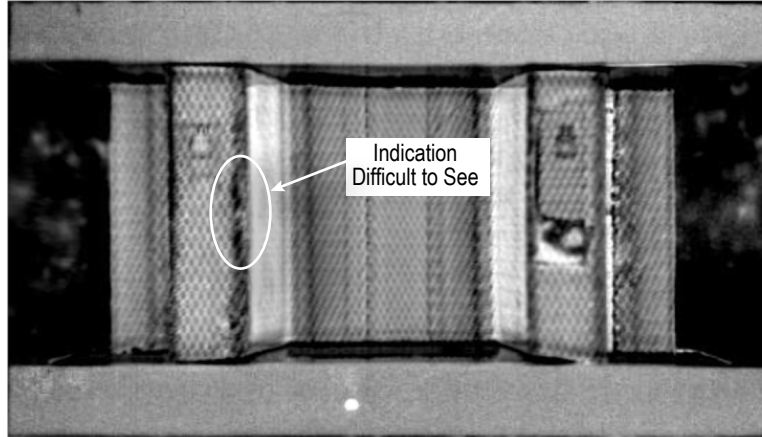
Figure 24. IRT for specimen double 7.

The specimen exhibited buckling of the face sheet beginning at 70 kips and failed catastrophically at 96.4 kips. Pictures of these two events are shown in figure 25. Since the crown did not fail as it did in specimen double 6, it is surmised that an impact at the crown/web interface is not as critical as an impact in the center of the crown. This is probably due to the high stiffness at the crown/web interface.
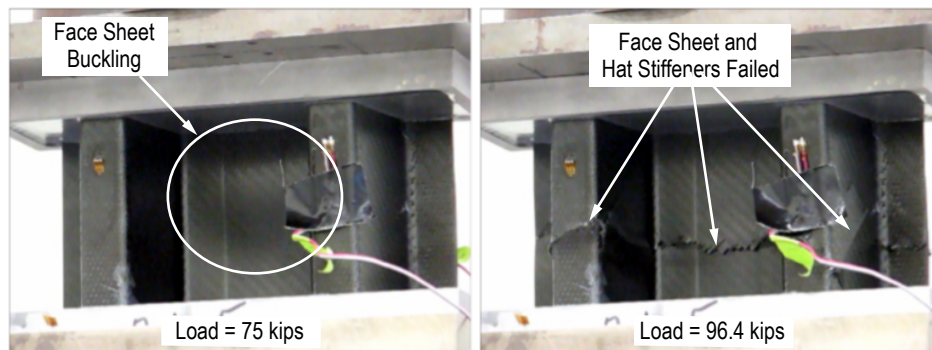
Figure 25. Buckling and catastrophic failure of specimen double 7.

3.1.8 Double 8.

This specimen was impacted on the face sheet from the rear at the midpoint between hat stiffeners with a 0.5-in-diameter impactor with an impact energy of 9.9 ft-lb as shown schematically in figure 26.
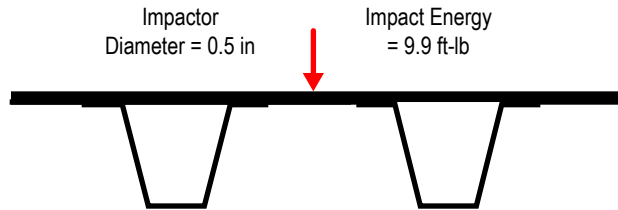

Figure 26. Location of impact on specimen double 8.

A photograph of an IRT image of the impacted specimen is presented in figure 27. The impact produced a circular area of damage ≈1 inch in diameter. This is similar to the damage produced by impacting the face sheet under a hat stiffener (specimen double 5).
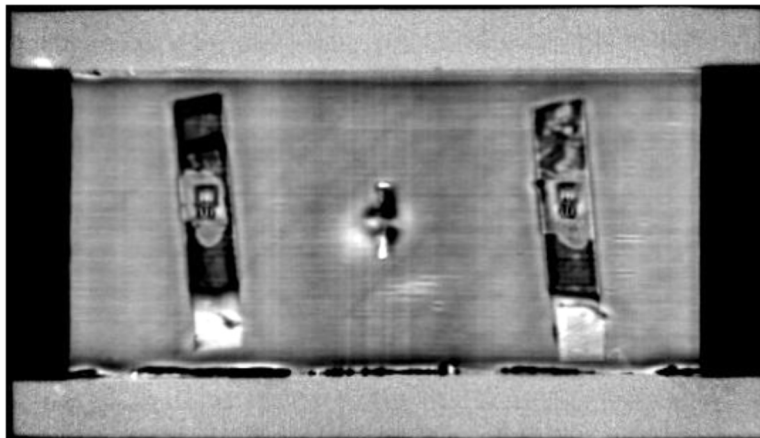
Figure 27. IRT for specimen double 8.

At a load of 69.3 kips, the face sheet of the specimen failed as shown in figure 28. Despite having a similar NDE signature as specimen double 5, this specimen demonstrated more residual compressive load-carrying capability. This is due to the co-cured, hat stiffener specimens demonstrating superior compression strength over the specimens with precured hat stiffeners.
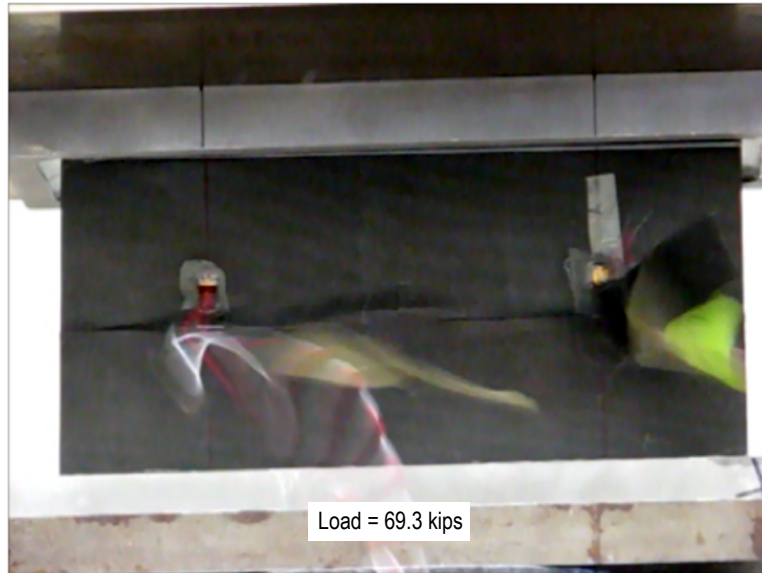
Figure 28. Failure of face sheet of specimen double 8.

The specimen was still able to carry a load of 36 kips as the hat stiffeners did not fail as shown in the post-testing picture in figure 29.
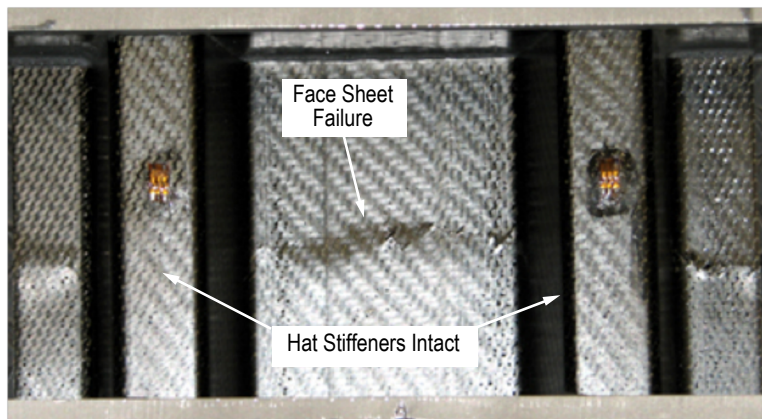
Figure 29. Specimen double 8 showing intact hat stiffeners after face sheet failure.

3.1.9 Double 9

This specimen was impacted on the face sheet behind a foot of one of the hat stiffeners with a 0.5-in-diameter impactor with an impact energy of 10.8 ft-lb as shown schematically in figure 30.
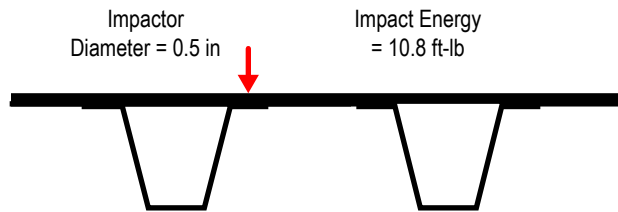

Figure 30. Location of impact on specimen double 9.

A photograph of an IRT image of the impacted specimen is presented in figure 31. The damage is about twice as long as it is wide, indicating that perhaps the impact caused a disbond of the foot from the face sheet (like specimen double 2).
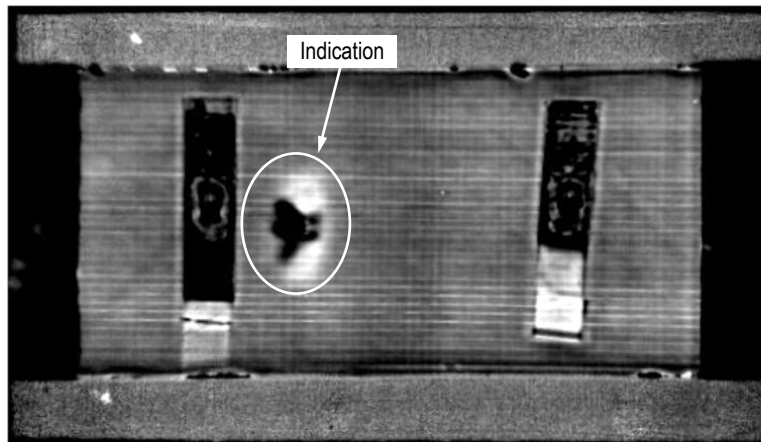

Figure 31. IRT for specimen double 9.

The specimen exhibited debonding of the foot from the face sheet at the impact site beginning at 50 kips. This event was not captured on video since all views during loading were from the impacted side. At a load of 54.1 kips, the specimen face sheet failed and the specimen held a residual load of 31.9 kips. As with specimen double 2, the residual load-carrying capability is due to the fact that the hat stiffeners did not fail and could thus carry load. A post-testing picture of specimen double 9 is shown in figure 32.
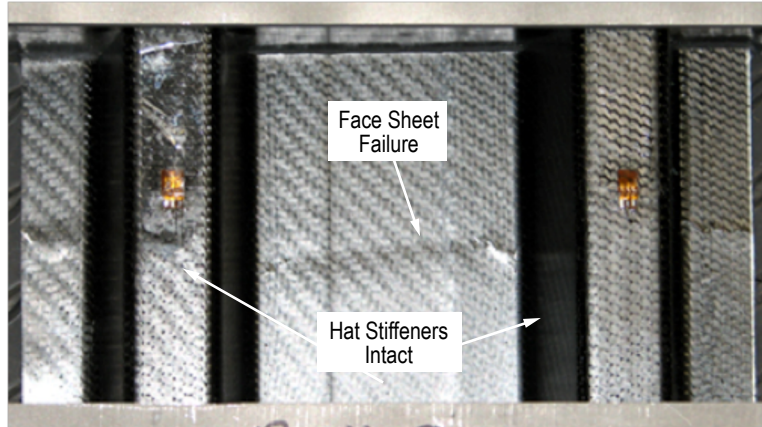
Figure 32. Specimen double 9 showing intact hat stiffeners after face sheet failure.

3.1.10 Double 10

This specimen was impacted on the face sheet directly behind one of the 'noodles' with a 0.5-in-diameter impactor with an impact energy of 10 ft-lb as shown in figure 33.
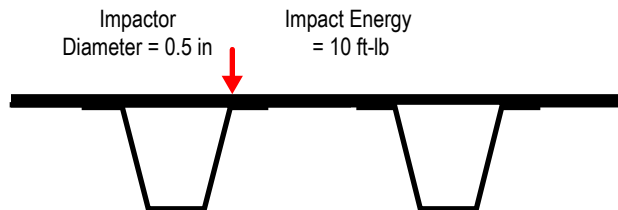

Figure 33. Location of impact on specimen double 10.

A photograph of an IRT image of the impacted specimen is presented in figure 34. The damage is approximately circular with a diameter of 0.5 in. This damage size is smaller than other impacts of similar energy. This is due to the face sheet being most stiff (transversely) where the hat stiffener meets the face sheet.
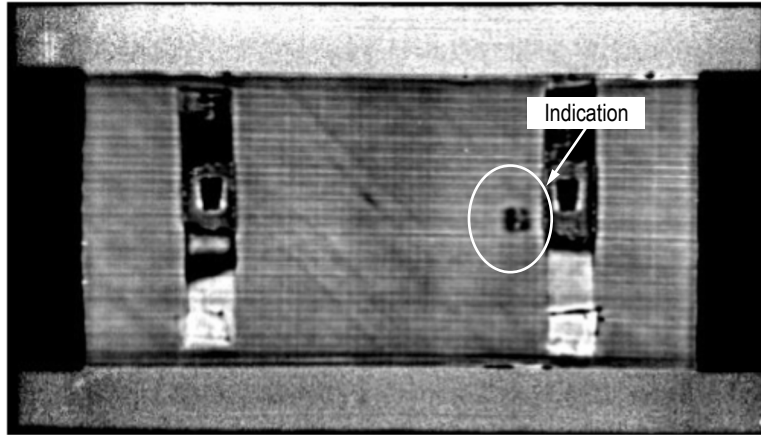
Figure 34. IRT for specimen double 10.

At a load of 91.7 kips, the specimen failed catastrophically. The face sheet did demonstrate buckling at ≈70 kips, but this was not as detectable by video when viewed from the face sheet side of the specimen. A photograph of the specimen just after failure is shown in figure 35. Unlike specimens that could carry a residual load after face sheet failure, this specimen demonstrated catastrophic failure as the hat stiffeners broke at the same time as the face sheet. A post-test picture of the specimen is shown in figure 36, showing the failed hat stiffeners in addition to the failed face sheet.
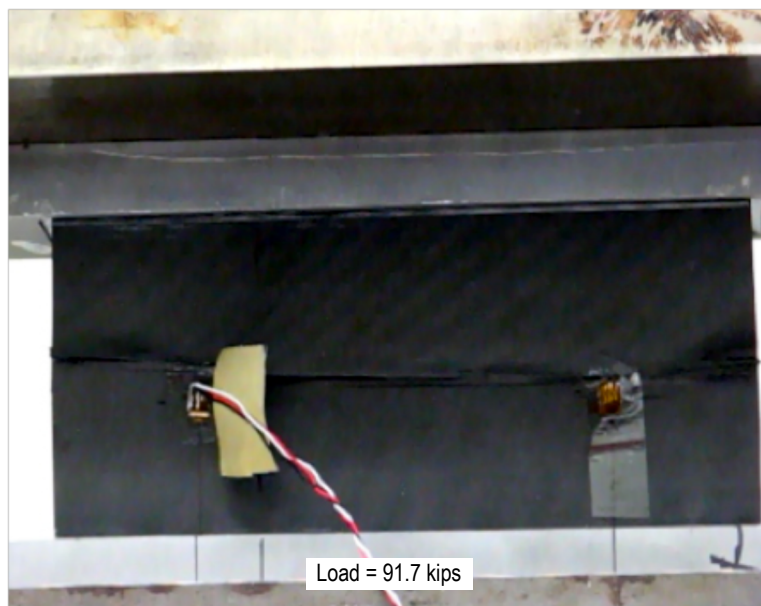
Figure 35. Failure of face sheet of specimen double 10.
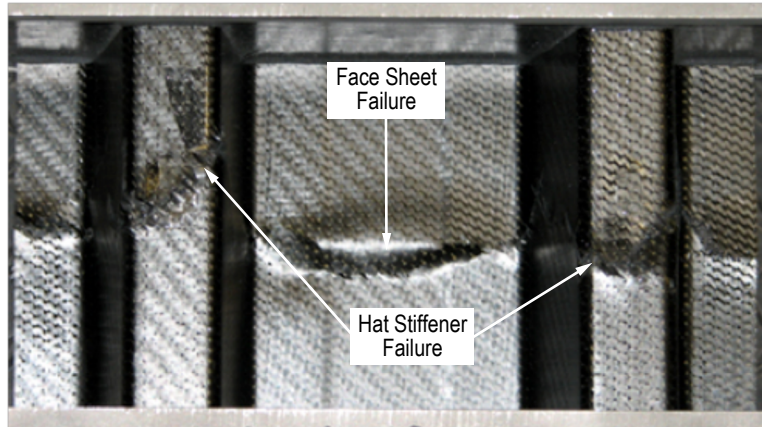
Figure 36. Specimen double 10 showing failed hat stiffeners and face sheet.

3.1.11 Double 11

This specimen was impacted identically to specimen double 10. Impact was on the face sheet directly behind one of the 'noodles' with a 0.5-in-diameter impactor with an impact energy of 10 ft-lb as shown in figure 37.
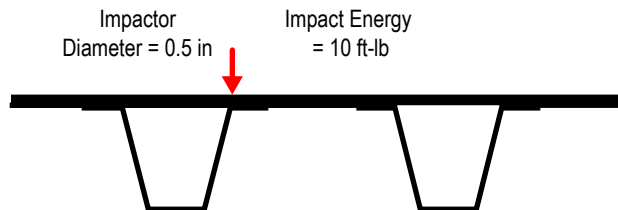

Figure 37. Location of impact on specimen double 11.

A photograph of an IRT image of the impacted specimen is presented in figure 38. As expected, this IRT image is similar to the IRT image of specimen double 10.
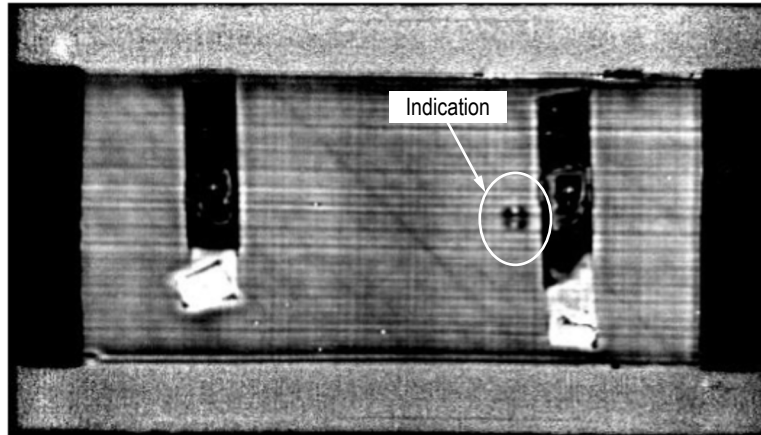
Figure 38. IRT for specimen double 11.

Buckling was seen at ≈75 kips and localized failure at the impact zone was noted at 83 kips. At a load of 85.7 kips, the specimen failed catastrophically. The only difference between the failure modes of specimen double 10 and specimen double 11 was that specimen double 11 exhibited preliminary failure before catastrophic break. The ultimate load was 7% lower in specimen double 11.

3.1.12 Double 12

This specimen was impacted on one of the crowns with a 0.5-in-diameter impactor with an impact energy of 10 ft-lb as shown schematically in figure 39. This impact was similar to the impact on specimen double 6, the main difference being that the impact energy used on specimen double 12 was 70% larger than that used on specimen double 6.
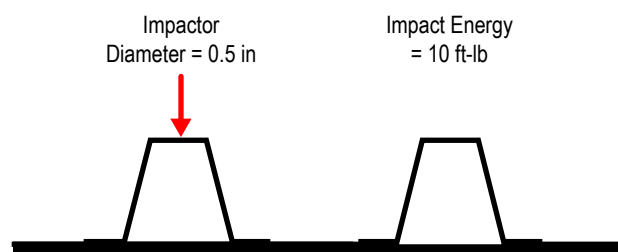
Figure 39. Location of impact on specimen double 12.

A photograph of an IRT image of the impacted specimen is presented in figure 40. As expected, this IRT image shows more damage in the crown than the impacted crown on specimen double 7. The damage covers the width of the crown and is 2.8 in long compared to 60% of the width of the crown and a length of 1 in.
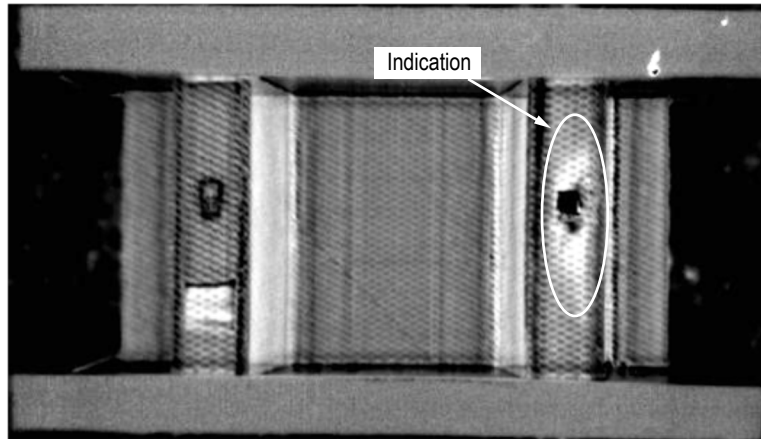
Figure 40. IRT for specimen double 12.

The impacted crown demonstrated a compressive failure at 50 kips. This event is shown in figure 41. The face sheet began a noticeable buckle at ≈60 kips and at a load of 77.8 kips, the specimen failed catastrophically. Photographs of these two events are shown in figure 42.
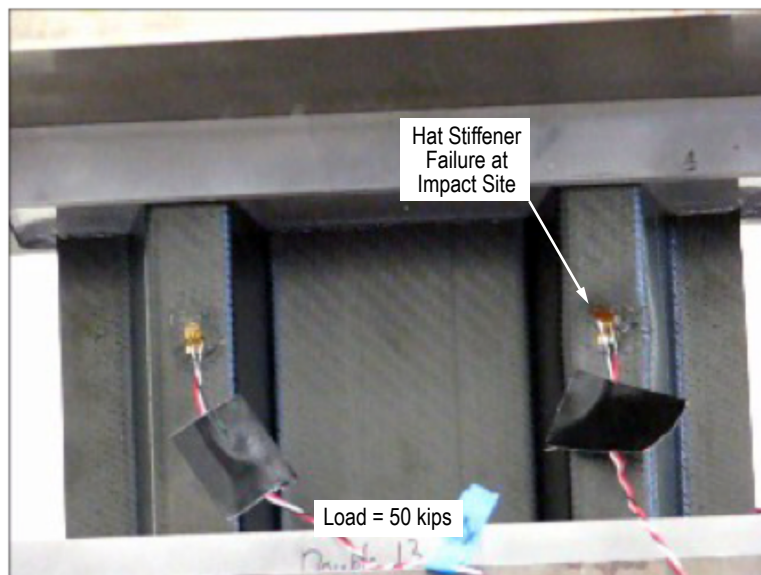
Figure 41. Dimpling at impact site and face sheet failure of specimen double 12.
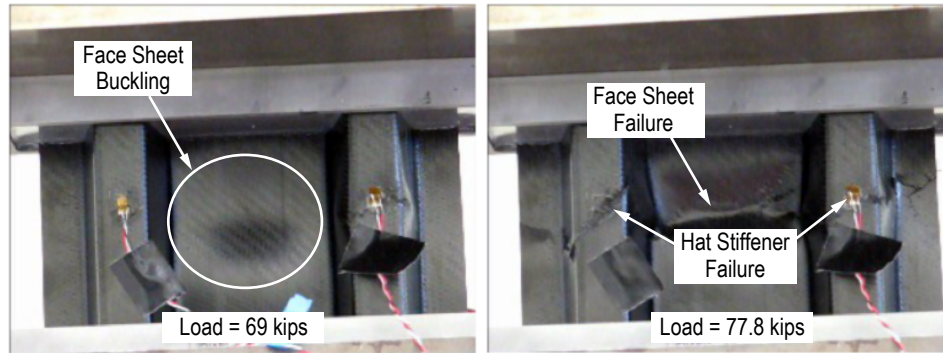
Figure 42. Face sheet buckling and catastrophic failure of specimen double 12.

3.1.13 Double 13

This specimen was impacted on the face sheet between the two hats with a 0.5-in-diameter impactor with impact energy of 10 ft-lb as shown schematically in figure 43. This impact is similar to that on specimen double 3, however, that specimen was manufactured with precured face sheets and hit with 44% less impact energy.
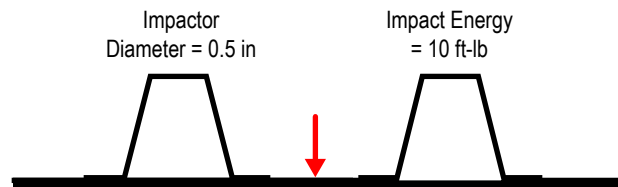
Figure 43. Location of impact on specimen double 13.

A photograph of an IRT image of the impacted specimen is presented in figure 44. The IRT image for this specimen is larger than that on specimen double 3, which is expected since this specimen was hit in the same location but with more impact energy.
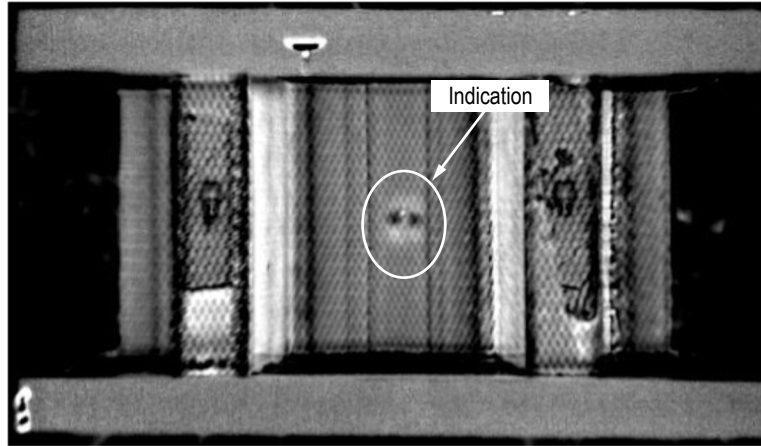
Figure 44. IRT for specimen double 13.

At a load of 64.4 kips, the face sheet failed but the hat stiffeners stayed intact and the specimen carried a residual load of 35 kips. A photograph of specimen double 13 after face sheet failure is shown in figure 45.
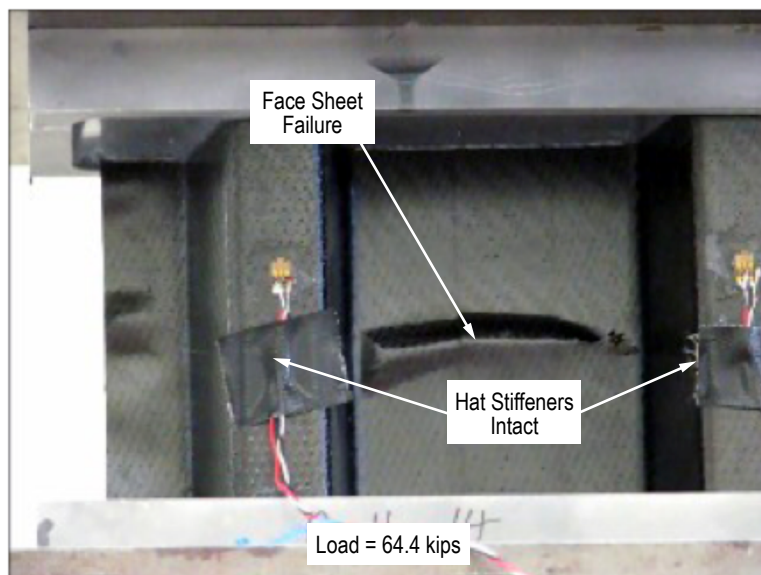
Figure 45. Face sheet failure of specimen double 13.

3.1.14 Double 14

This specimen was impacted on the face sheet from the rear, directly between the two hat stiffeners with a 0.5-in-diameter impactor with impact energy of 10 ft-lb as shown schematically in figure 46. This impact was very similar to the impact inflicted upon specimen double 8.
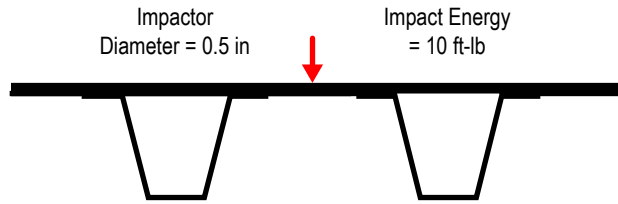
Figure 46. Location of impact on specimen double 14.

A photograph of an IRT image of the impacted specimen is presented in figure 47. As expected, this IRT image is similar to the IRT image of specimen double 8, though slightly larger. The degree of damage seen in specimen double 14 is 1.1 in wide compared to a 0.9-in width for specimen double 8.

Localized dimpling at the impact zone was noted at 45 kips. At a load of 51.2 kips (26% lower than specimen double 8), the specimen failed, but continued to carry a load of 29 kips. Pictures of these two events are shown in figure 48.
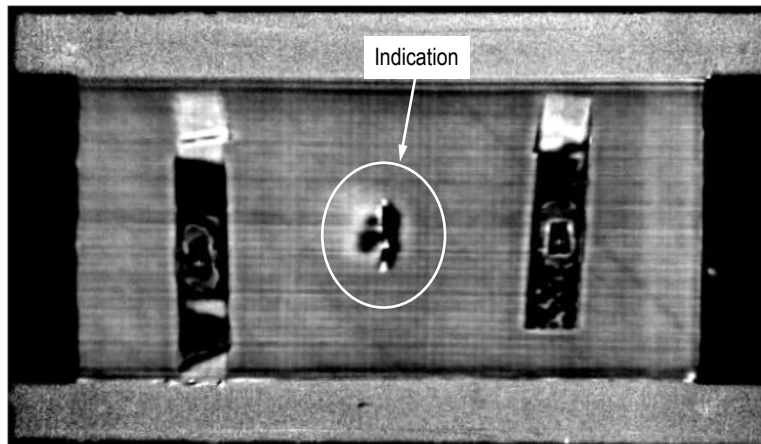
Figure 47. IRT for specimen double 14.
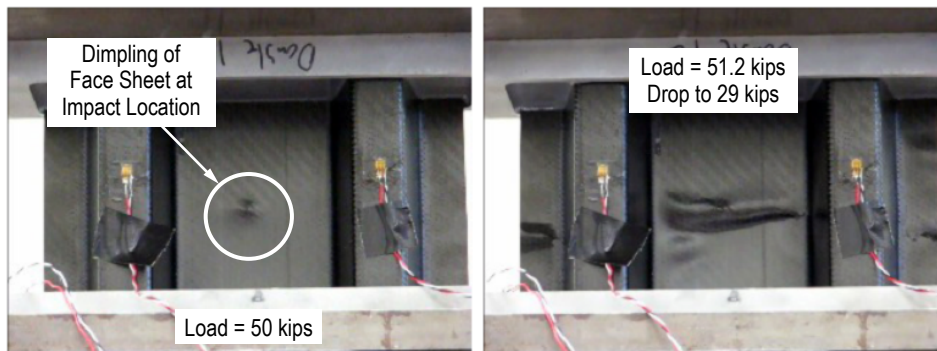
Figure 48. Dimpling at impact site and face sheet failure of specimen double 14.

Upon continued loading, the specimen then reached 37 kips before the load dropped again. This specimen demonstrated a similar failure mode but had less compressive load-carrying capability than specimen double 8. Upon closer inspection of the video recordings, it was noted that specimen double 14 had an audible cracking sound at the onset of the formation of the dimple at the impact site (45 kips). When specimen double 8 failed, there were no audible sounds before the face sheet failure. This indicates that specimen double 14 had less interlaminar strength in its face sheet than specimen double 8. This hypothesis was supported upon continued loading of specimen double 14 in which further delaminations formed in the face sheet rather than the load being effectively transferred to the hat stiffeners.

Later in the program it was confirmed that specimen double 14 came from a batch of specimens that all exhibited early face sheet delaminations, so much that the results of the CAI tests on this batch of specimens could not be included in this study since there was an obvious processing problem.

A summary of the hat-stiffened specimens is given in table 1. The impact energy for each specimen has been divided by the thickness of the laminate at the section of panel that was impacted. For example, all impacts on the crown portion of a specimen had their energies divided by 0.15 in, and all impacts on the face sheet portion of a specimen had their energies divided by 0.11 in.

The CAI strength is given as load per unit length; i.e., the failure load divided by 8.875 in. The specimens in bold were co-cured.

The data in table 1 are represented graphically in figure 49. A curve fit or other type of data comparison is not possible since the impacts were in different locations on the hat-stiffened panel, which completely change the damage mechanics involved. The data of the co-cured, hat-stiffened panels on the plot are noted as to what part of the specimen the impact took place at.

Table 1. Summary of CAI results on hat-stiffened specimens.

| Specimen	Impact Energy	CAI Strength (in-lb/in)
Double 1	0	7,500
Double 2	602	6,600
Double 3	609	6,600
Double 4	682	5,000
Double 5	1,094	5,800
Double 6	472	9,500
Double 7	617	10,900
Double 8	1,082	7,800
Double 9	1,178	6,100
Double 10	1,091	10,300
Double 11	1,091	9,700
Double 12	800	8,800
Double 13	1,088	7,300
Double 14*	1,091	5,800

*Poorly processed specimen
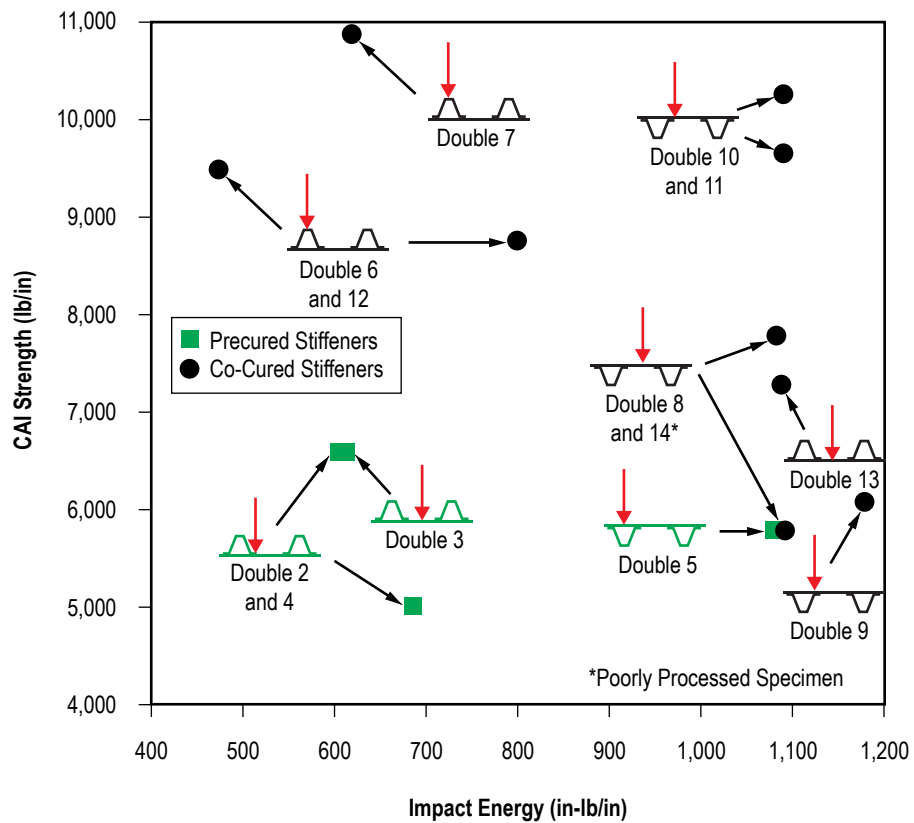
Figure 49. Residual strength versus impact energy for hat-stiffened specimens.

3.2 Sandwich Specimens

The CAI test results of the sandwich panels to be compared to the hat-stiffened panel are summarized in table 2. The impact energy has been divided by the thickness of the impacted face sheet (0.10 in) in order to produce more comparable numbers for comparison with the hat-stiffened specimens. The CAI strength is given as a line load; i.e., the total failure load was divided by the specimen width.

Table 2. CAI results for sandwich specimens used in this study.

Specimen	Impact Energy	CAI Strength (lb/in)
Sandwich 1	1,140	9,900
Sandwich 2	876	11,300
Sandwich 3	648	12,900
Sandwich 4	636	13,200
Sandwich 5	1,140	9,700
Sandwich 6	1,224	11,000
Sandwich 7	1,536	9,500
Sandwich 8	1,536	10,200
Sandwich 9	876	12,600
Sandwich 10	432	13,900
Sandwich 11	468	13,800
Sandwich 12	528	12,100
Sandwich 13	720	12,600
Sandwich 14	768	12,600
Sandwich 15	840	11,700
Sandwich 16	324	15000
Sandwich 17	1,008	11,500
Sandwich 18	648	13,800
Sandwich 19	852	12,100
Sandwich 20	1,572	10,900
Sandwich 21	1,992	9,000
Sandwich 22	1,116	11,700
Sandwich 23	864	12,300
Sandwich 24	768	12,900

The data in table 2 are represented graphically in figure 50. A power curve is fitted to the data since the impacts for these specimens were independent of location; i.e., the sandwich structure is continuous.

As a comparison of the CAI strength versus damage severity for the hat-stiffened panels and the sandwich panels, the plots in figures 49 and 50 are combined and presented in figure 51.

31
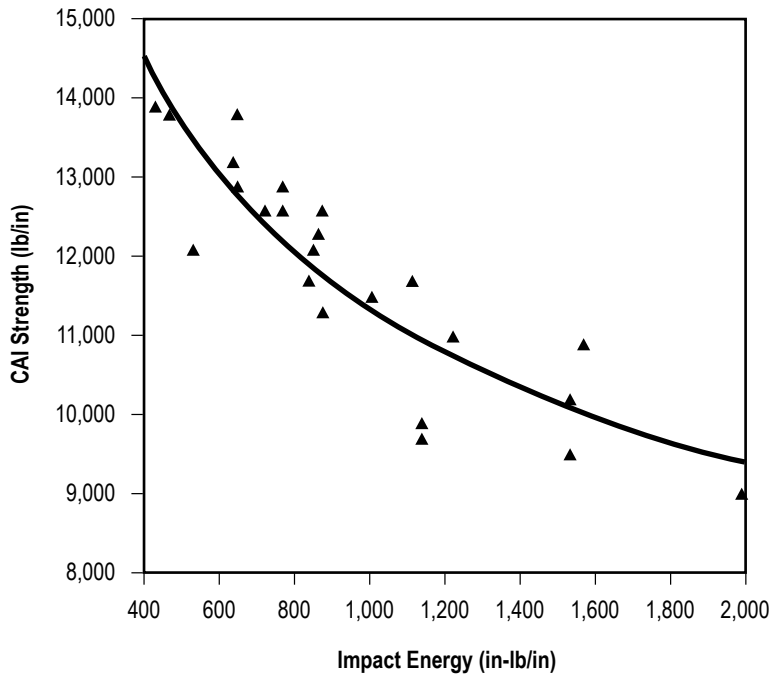
Figure 50. Residual strength versus impact energy sandwich specimens.

Since the hat-stiffened panels had a smaller areal weight than the sandwich panels, the data in figure 51 can be normalized for a better comparison of strength-to-weight ratios of the two types of panel construction. The hat-stiffened CAI data are divided by 1.76 lb/ft^2 and the sandwich CAI data are divided by 2.34 lb/ft^2.
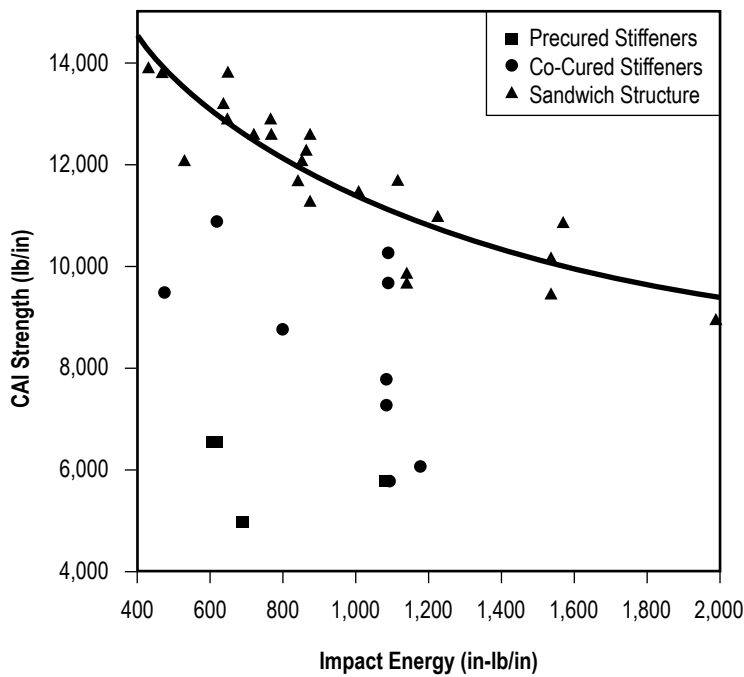
Figure 51. Comparison of hat-stiffened and sandwich specimens.

A comparison of the sandwich and hat-stiffened CAI data, taking mass of the structure into consideration (strength-to-weight ratio), is shown in figure 52.
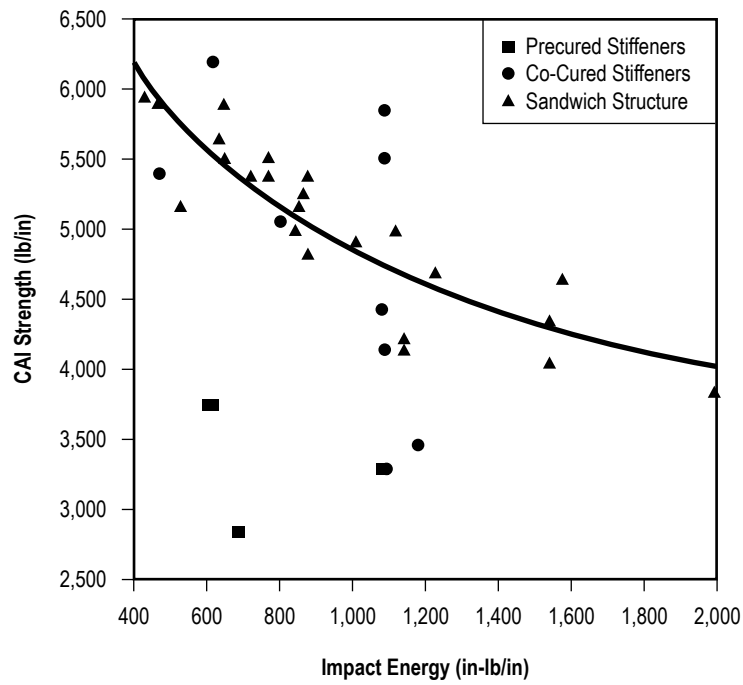
Figure 52. Comparison of hat-stiffened and sandwich
specimens with mass of structure included.

4. DISCUSSION

4.1 Co-Cured Versus Precured Hat-Stiffened Specimens

Specimens double 1–5 were manufactured with the hat stiffeners procured and bonded onto the face sheet in a secondary bonding operation. All other hat-stiffened specimens had the stiffeners and face sheet co-cured in one bonding/curing operation. The co-curing of the hats to the face sheet obviously results in a higher load-carrying structure as relatively undamaged specimens carried 84.7, 96.4, 91.7, and 85.7 kips while an undamaged specimen manufactured by secondarily bonding the hats to the face sheet (double 1) failed at 66.6 kips.

4.2 Size of Impactor

Although only two specimens where impacted with an impactor of size other than 0.5 inches in diameter, some observations can be made. For the procured, hat-stiffened specimens, double 2 and double 4 were both impacted on a foot of a hat stiffener. Specimen double 2 was impacted with an impactor of 0.5-in diameter and specimen double 4 was hit with a 1.5-in-diameter impactor. When the impactor size was increased to 1.5 in diameter (and impacted with slightly more impact energy), an impact on the foot of a hat caused the residual load-carrying capability of the structure to be reduced from 58 to 44.4 kips. The IRT results show that the larger impactor caused a larger disbond between the impacted foot and the face sheet and compression testing revealed that the disbond caused from the larger impactor was actually within the face sheet rather than at the hat stiffener/face sheet interface. In the only other test utilizing an impactor size of 1.5-in, co-cured specimen double 7 was impacted at the edge of a crown. This impact did not reduce the residual compression load-carrying capability of the specimen, thus no valid comparisons regarding impactor size can be made.

4.3 Location of Impact

For the co-cured, hat-stiffened specimens, impacting the face sheet directly behind one of the noodles did not cause much strength reduction in the specimen. This is probably due to this area being very transversely stiff and thus the impact consists almost solely of contact stresses, which did not cause damage that was detrimental to the residual load-carrying capability of the specimen. For an impact on the edge of a hat stiffener, another highly transversely stiff area, the residual load-carrying capability, was also not greatly diminished. Impacting a hat stiffener in the center of the hat did cause a modest reduction in the load-carrying capability of the specimen when hit with sufficient energy; however, the failure mode was in two distinct phases. First, the impacted hat stiffener failed but the specimen continued to carry load until ultimate failure. Impacts on the face sheet or face sheet/hat stiffener interface apparently caused the greatest reduction in residual compressive load-carrying capability.

4.4 Comparison With Sandwich Panels

In order to better compare these hat-stiffened specimens to sandwich structure specimens, the mass per unit area of each type of structure was assessed. The double hat specimens had an average mass of 0.65 lb$_m$. Since these specimens were 6 in high and 8.875 in wide, this gives an areal density of 1.76 lb/ft^2. Sandwich panel used in this study had an areal density of 2.34 lb/ft^2. The hat structure is thus 25% lighter than the sandwich structure that it will be compared to. Figure 49 shows compressive line load that the structures could carry versus impact energy. The double hat specimens are divided out between the secondarily bonded hat type (CAI Pre) and the co-cured hat type (CAI Co).

Note that the hat specimens are much more dependent upon where on the structure the impact occurs. The sandwich structure is uniform across its surface so all impacts on the surface are identical.

Once the residual compressive load-carrying capability of the specimens is normalized by the areal weight of the specimens, it appears that the hat specimens can carry more load after an impact event of a given energy with a spherical impactor as shown in figure 52.

5. CONCLUSIONS

From the data generated in this study, it appears that the compressive load-carrying ability of hat-stiffened and sandwich structure of the type considered for a launch vehicle interstage is comparable for a well-made structure when damage tolerance is considered. However, other factors such as inspectability and failure mode will also need to be addressed in a full damage tolerance study.

Since the hat-stiffened structure demonstrated redundancy in its design (load redistribution after a localized failure), it would be classified as a more 'damage tolerant' structure by most standards. For example, if this study was examining airplane fuselage structure, then the step-wise failure mode of the hat-stiffened structure would be most desirable as the fuselage can still carry a significant amount of ultimate load after initial localized failure, allowing for the airplane to land using 'get home loads.' However, for a launch vehicle, this step-wise failure mode has no benefits since the rocket cannot shut down once launched, thus the ultimate load-carrying capability is of interest.

With the limited data thus far, it is difficult to draw definitive conclusions about the damage tolerance aspects of the hat-stiffened structure. However, it does appear that, in general, an impact on the face sheet of a hat structure is more detrimental than an impact on the hat stiffener of the structure (as was found in ref. 4). An exception is when the impact is over the noodle of a hat, in which case, little detrimental effect to compression strength was seen at 10 ft-lb of impact energy.

Further testing over a broader range of impact energies is planned for the next round of testing.

REFERENCES

1. Gadke, M.; Geier, B.; Goetting, H.; et al.: "Damage Influence on the Buckling Load of CFRP Stringer-Stiffened Panels," *Composite Structures*, Vol. 36, pp. 249–275, 1996.

2. Abrate, S.: "Localized Impact on Sandwich Structures With Laminated Facings," *Applied Mechanics Reviews,* Vol. 50, pp. 69–83, 1997.

3. Rhodes, M.D.; Williams, J.G.; and Starnes, J.H.: "Effect of Low-Velocity Impact Damage on the Compressive Strength of Graphite-Epoxy Hat-Stiffened Panels," *NASA TN D-8411*, 1997.

4. Ambur, D.R.: "Design and Evaluation of a Foam-Filled Hat-Stiffened Panel Concept for Aircraft Primary Structural Applications," *NASA TM 109175*, NASA Langley Research Center, Hampton, VA, 1995.

5. Ambur, D.R.; and Dexter, B.H.: "Structural Performance of a Compressively Loaded Foam-Core Hat-Stiffened Textile Composite Panel," *NASA TM-111451*, NASA Langley Research Center, Hampton, VA, 1966.

6. Rousseau, C.Q.; Baker, D.J.: and Hethcock, J.D.: "Parametric Study of Three-Stringer Panel Compression-After-Impact Strength," *Composite Structures: Theory and Practice, ASTM STP 1383*, P. Grant and C.Q. Rousseau (eds.), American Society for Testing and Materials, West Conshohocken, PA, pp. 72–104, 2000.

7. Bisagni, C.; Vescovini, R.; and Davila, C.G.: "Assessment of the Damage Tolerance of Postbuckled Hat-Stiffened Panels using Single-Stringer Specimens," *Proceedings 51st AIAA/ASME/ASCE/AHS/ASC Structures, Structural Dynamics and Materials Conference*, Orlando, FL, USA, April 12–15, 2010.

8. Nettles, A.T.; and Jackson, J.R.: "Developing a Material Strength Design Value Based on Compression After Impact Damage for the ARES I Composite Interstage," *NASA/TP—2009–215634*, Marshall Space Flight Center, AL, 2009.

REPORT DOCUMENTATION PAGE

Form Approved
OMB No. 0704-0188

1. REPORT DATE *(DD-MM-YYYY)* 01–12–2011	2. REPORT TYPE Technical Memorandum	3. DATES COVERED *(From - To)*

4. TITLE AND SUBTITLE

A Damage Tolerance Comparison of Composite Hat-Stiffened and Honeycomb Sandwich Structure for Launch Vehicle Interstage Applications

5a. CONTRACT NUMBER

5b. GRANT NUMBER

5c. PROGRAM ELEMENT NUMBER

6. AUTHOR(S)

A.T. Nettles

5d. PROJECT NUMBER

5e. TASK NUMBER

5f. WORK UNIT NUMBER

7. PERFORMING ORGANIZATION NAME(S) AND ADDRESS(ES)

George C. Marshall Space Flight Center
Huntsville, AL 35812

8. PERFORMING ORGANIZATION REPORT NUMBER

M–1326

9. SPONSORING/MONITORING AGENCY NAME(S) AND ADDRESS(ES)

National Aeronautics and Space Administration
Washington, DC 20546–0001

10. SPONSORING/MONITOR'S ACRONYM(S)

11. SPONSORING/MONITORING REPORT NUMBER

NASA/TM—2011–216477

12. DISTRIBUTION/AVAILABILITY STATEMENT

Unclassified-Unlimited
Subject Category 24
Availability: NASA CASI (443–757–5802)

13. SUPPLEMENTARY NOTES

Prepared by the Materials & Processes Laboratory, Engineering Directorate

14. ABSTRACT

In this study, a direct comparison of the compression-after-impact (CAI) strength of impact-damaged, hat-stiffened and honeycomb sandwich structure for launch vehicle use was made. The specimens used consisted of small substructure designed to carry a line load of ≈3,000 lb/in. Damage was inflicted upon the specimens via drop weight impact. Infrared thermography was used to examine the extent of planar damage in the specimens. The specimens were prepared for compression testing to obtain residual compression strength versus damage severity curves. Results show that when weight of the structure is factored in, both types of structure had about the same CAI strength for a given damage level. The main difference was that the hat-stiffened specimens exhibited a multiphase failure whereas the honeycomb sandwich structure failed catastrophically.

15. SUBJECT TERMS

impact, compression-after-impact (CAI), skin-stiffened, honeycomb sandwich, damage tolerance, impact damage

16. SECURITY CLASSIFICATION OF:			17. LIMITATION OF ABSTRACT	18. NUMBER OF PAGES	19a. NAME OF RESPONSIBLE PERSON STI Help Desk at email: help@sti.nasa.gov
a. REPORT	**b. ABSTRACT**	**c. THIS PAGE**	UU	52	
U	U	U			**19b. TELEPHONE NUMBER** *(Include area code)* STI Help Desk at: 443–757–5802

Standard Form 298 (Rev. 8-98)
Prescribed by ANSI Std. Z39-18

National Aeronautics and
Space Administration
IS20
George C. Marshall Space Flight Center
Huntsville, Alabama 35812